1521-0111/12/8205-972–982$25.00
MOLECULAR PHARMACOLOGY
Vol. 82, No. 5
80853/3803240

Mol Pharmacol 82:972–982, 2012

α-Conotoxin PeIA[S9H,V10A,E14N] Potently and Selectively Blocks α6β2β3 versus α6β4 Nicotinic Acetylcholine Receptors[S]

Arik J. Hone, Mick'l Scadden, Joanna Gajewiak, Sean Christensen, Jon Lindstrom, and J. Michael McIntosh

Department of Biology (A.J.H., M.S., J.G., S.C., J.M.M.), Interdepartmental Program in Neuroscience (J.M.M.), and Department of Psychiatry (J.M.M.), University of Utah, Salt Lake City, Utah; and Department of Neuroscience, University of Pennsylvania Medical School, Philadelphia, Pennsylvania (J.L.)

Received June 27, 2012; accepted August 17, 2012

ABSTRACT

Nicotinic acetylcholine receptors (nAChRs) containing α6 and β2 subunits modulate dopamine release in the basal ganglia and are therapeutically relevant targets for treatment of neurological and psychiatric disorders including Parkinson's disease and nicotine dependence. However, the expression profile of β2 and β4 subunits overlap in a variety of tissues including locus ceruleus, retina, hippocampus, dorsal root ganglia, and adrenal chromaffin cells. Ligands that bind α6β2 nAChRs also potently bind the closely related α6β4 subtype. To distinguish between these two subtypes, we synthesized novel analogs of a recently described α-conotoxin, PeIA. PeIA is a peptide antagonist that blocks several nAChR subtypes, including α6/α3β2β3 and α6/α3β4 nAChRs, with low nanomolar potency. We systematically mutated PeIA and evaluated the resulting analogs for enhanced potency and/or selectivity for α6/α3β2β3 nAChRs expressed in *Xenopus* oocytes (α6/α3 is a subunit chimera that contains the N-terminal ligand-binding domain of the α6 subunit). On the basis of these results, second-generation analogs were then synthesized. The final analog, PeIA[S9H,V10A,E14N], potently blocked acetylcholine-gated currents mediated by α6/α3β2β3 and α6/α3β4 nAChRs with IC_{50} values of 223 pM and 65 nM, respectively, yielding a >290-fold separation between the two subtypes. Kinetic studies of ligand binding to α6/α3β2β3 nAChRs yielded a k_{off} of 0.096 ± 0.001 min^{-1} and a k_{on} of 0.23 ± 0.019 min^{-1} M^{-9}. The synthesis of PeIA[S9H,V10A,E14N] demonstrates that ligands can be developed to discriminate between α6β2 and α6β4 nAChRs.

Introduction

Mammalian neuronal nicotinic acetylcholine receptors (nAChRs) assemble in a pentameric stoichiometry from eight α and three β subunits to form various receptor subtypes. Selective ligands have played a critical role in identifying individual subtypes and defining their physiological functions. nAChR subtypes that contain the α6 subunit have a very restricted tissue distribution. In the central nervous system, α6-containing nAChRs are expressed in dopaminergic regions including the substantia nigra, ventral tegmental area, and nucleus accumbens (Yang et al., 2009; Gotti et al., 2010). Dopaminergic neurons of the substantia nigra are gradually lost in Parkinson's disease, which leads to disordered control over motor movement (Bordia et al., 2007). In reward centers of the brain, activation of α6-containing nAChRs enhances dopamine release and reinforces the addictive properties of nicotine (Pons et al., 2008; Jackson et al., 2009; Brunzell et al., 2010; Exley et al., 2011; Liu et al., 2012). In these midbrain areas, α6 subunits assemble with β2 subunits to form α6β2* nAChRs (asterisk denotes the possible presence of additional subunits), areas where expression of the β4 subunit is minimal or absent, and, therefore, few, if any, α6β4* nAChRs are likely to be present. Thus, ligands that bind α6* nAChRs can be used in these regions to selectively identify α6β2* nAChRs. However, in other areas such as the retina (Moretti et al., 2004; Marritt et al., 2005) and the locus ceruleus (Léna et al., 1999; Vincler and Eisenach, 2003; Azam and McIntosh, 2006), α6β4*

This work was supported by the National Institutes of Health National Institute of General Medical Sciences [Grants GM48677, GM103801]; and National Institutes of Health National Institute of Neurological Disorders and Stroke [Grant NS1132].
Article, publication date, and citation information can be found at http://molpharm.aspetjournals.org.
http://dx.doi.org/10.1124/mol.112.080853.
[S] The online version of this article (available at http://molpharm.aspetjournals.org) contains supplemental material.

ABBREVIATIONS: nAChR, nicotinic acetylcholine receptor; α-Ctx, α-conotoxin; ACh, acetylcholine; Fmoc, 9-fluorenylmethyloxycarbonyl; HPLC, high-performance liquid chromatography.

nAChRs are present and may be coexpressed with the α6β2* subtype. Moreover, in the hippocampus of mouse, α6β4* nAChRs control the release of norepinephrine (Azam et al., 2010). Last, in the peripheral nervous system, α6β4* nAChRs are expressed by human adrenal chromaffin cells (Pérez-Alvarez et al., 2012) and by rat dorsal root ganglion neurons (Hone et al., 2012), two cell populations that also have substantial β2 subunit expression. Thus, ligands that can discriminate between α6β2* and α6β4* nAChRs are needed to facilitate the study of α6β2* nAChRs in areas where multiple α6-containing nAChRs are potentially expressed.

Predatory cone snails (*Conus*) have evolved a rich, combinatorial-like library of neuropharmacologically active compounds. Among the principal components of the cone snail venom are the α-conotoxins (α-Ctxs), disulfide-rich peptide antagonists of nAChRs. Each species of cone snail produces several distinct α-Ctxs as part of its venom arsenal to immobilize prey. Subsets of these α-Ctxs are now widely used by neuroscientists to block the function of mammalian nAChR subtypes (Azam and McIntosh, 2009; Armishaw, 2010). However, as the diversity of nAChR subtypes is progressively elucidated, the need for increasingly selective ligands correspondingly grows. Several existing α-Ctxs potently block α6 nAChRs. However, α-Ctxs that block α6/α3β2β3 nAChRs also potently block α6/α3β4 nAChRs (Dowell et al., 2003). Thus, further refinement of the specificity of these ligands is required.

α-Ctx PeIA, cloned from a cDNA library of *Conus pergrandis,* potently blocks several nAChRs subtypes including those that contain the α6 subunit (McIntosh et al., 2005). We used α-Ctx PeIA as a template to create ligands with novel specificity and tested them on *Xenopus* oocytes expressing cloned nAChRs. We used rat and mouse α6/α3 subunit chimeras to model the α6β2 and α6β4 ligand-binding domain because injection of nonchimeric α6 with β2 and β3 fails to reliably produce functional expression (Kuryatov et al., 2000; Dowell et al., 2003; Papke et al., 2005; Dash et al., 2011). However, comparison of data obtained from studies on heterologously expressed chimeric constructs of α6 with studies on native α6-containing nAChRs demonstrate that these chimeric constructs and native α6-containing nAChRs share a similar pharmacological profile (Bordia et al., 2007; Capelli et al., 2011; Pérez-Alvarez et al., 2012). With use of this strategy and through synthetic iteration of α-Ctx PeIA, we created a ligand that to our knowledge is the most selective α-Ctx to date for distinguishing between α6β2β3 and α6β4 nAChRs.

Materials and Methods

Rat α3, α4, and α7 nAChR subunit clones were provided by S. Heinemann (Salk Institute for Biological Studies, San Diego, CA), C. Luetje (University of Miami, Miami, FL) provided the β2, β3, and β4 subunits in the high-expressing pGEMHE vector, and α9 and α10 were provided by A. Elgoyhen (Universidad de Buenos Aires, Buenos Aires, Argentina). Mouse α6, β2, β3, and β4 subunit clones were provided by J. Stitzel (University of Colorado, Boulder, CO). Construction of α6/α3 subunit chimeras has been described previously, they consist of an α3 subunit, in which the first 237 amino acids of the ligand-binding domain are replaced with the corresponding α6 amino acids (McIntosh et al., 2004). The rat α6/α4 chimera was provided by R. Papke (University of Florida, Gainesville, FL). These chimeras were used because of poor expression of the nonchimeric forms of the α6 construct. The human β3-α6-β2-α4-β2 concatamer has been described previously (Kuryatov and Lindstrom, 2011). Acetylcholine chloride (ACh) and bovine serum albumin were obtained from Sigma-Aldrich (St. Louis, MO). HEPES was purchased from Research Organics (Cleveland, OH).

Peptide Synthesis. Standard peptide chemistry was used to generate the α-Ctx peptides as described previously (Cartier et al., 1996), or the peptides were synthesized on an Apex 396 automated peptide synthesizer (AAPPTec, Louisville, KY), applying standard solid-phase 9-fluorenylmethyloxycarbonyl (Fmoc) methods. The peptides were initially constructed on Fmoc-Rink Amide MBHA resin (substitution: 0.4 mmol/g^{-1}; Peptides International Inc., Louisville, KY). All standard amino acids were purchased from AAPPTec. Side chain protection for the amino acids was as follows: His and Asn, trityl; and Ser, *tert*-butyl. Cys residues were orthogonally protected by trityl for Cys^1 and Cys^3 and acetamidomethyl for Cys^2 and Cys^4. The peptides were synthesized at a 50-μmol scale. Coupling activation was achieved with 1 equivalent of 0.4 M benzotriazol-1-yl-oxytripyrrolidinophosphonium hexafluorophosphate and 2 equivalents of 2 M *N,N*-diisopropylethyl amine in *N*-methyl-2-pyrrolidone as the solvent. For each coupling reaction a 10-fold excess of amino acid was used, and the reaction was conducted for 60 min. The Fmoc deprotection reaction was carried out for 20 min with 20% (v/v) piperidine in dimethylformamide. The peptides were cleaved from the resin using Reagent K (trifluoroacetic acid-phenol-1,2-ethanedithiol-thioanisol-H_2O; 9:0.75:0.25:0.5:0.5 by volume), and a two-step oxidation protocol was used to selectively fold the peptides in the correct disulfide configuration. In brief, the first disulfide bridge was closed using 20 mM potassium ferricyanide and 0.1 M Tris-HCl, pH 7.5. The solution was allowed to react for 45 min, and then the monocyclic peptide was purified by reverse-phase high-performance liquid chromatography (HPLC). Simultaneous removal of the acetamidomethyl groups and closure of the second disulfide bridge were performed by iodine oxidation. The monocyclic peptides in HPLC eluent were dripped into an equal volume of iodine (10 mM) in H_2O-trifluoroacetic acid-acetonitrile (78:3:25 by volume) and allowed to react for 10 min. The reaction was terminated by the addition of 1 M ascorbic acid diluted 20-fold with 0.1% (v/v) trifluoroacetic acid, and the bicyclic product was purified by reverse-phase HPLC. The masses of the peptides were verified by matrix-assisted laser desorption ionization/time-of-flight mass spectrometry at the Salk Institute for Biological Studies under the direction of Dr. J. Rivier. Mass spectrometry and HPLC data for the peptides are shown in Supplemental Table 1.

Two-Electrode Voltage-Clamp Electrophysiology of *Xenopus laevis* Oocytes. Detailed methods for conducting electrophysiological experiments of nAChRs heterologously expressed in *X. laevis* oocytes have been described in detail previously (Hone et al., 2009). In brief, stage IV to V oocytes were injected with equal ratios of cRNA encoding cloned rat and mouse nAChR subunits α3, α4, α6/α3, α7, α9, α10, β2, β3, and β4 and used 1 to 4 days after injection. The oocyte membranes were clamped at a holding potential of −70 mV and continuously gravity perfused with standard ND96 solution and stimulated with 1-s pulses of ACh once every minute. The solution changes were controlled through a series of three-way solenoid valves interfaced with a personal computer via a CoolDrive valve driver (Neptune Research and Development, West Caldwell, NJ) and LabVIEW software (National Instruments, Austin, TX). The ACh-gated currents (I_{ACh})were acquired using an Oocyte OC-725 series voltage-clamp amplifier (Warner Instruments, Hamden, CT), filtered through a 5-Hz low-pass Bessel style filter (model F1B1; Frequency Devices, Ottawa, IL), and digitized at 50 Hz using a National

Instruments USB-6009 digital to analog converter. The toxins were diluted in ND96, and perfusion was applied up to 1 μM; concentrations $\geq$10 μM were bath-applied in a static bath for 5 min. To determine the observed off rates (k_{off}), the toxins were applied at 10 or 100 μM, depending on the nAChR subtype and the potency of the toxin. PeIA, PeIA[V10], and PeIA[E14N] were applied at 100 μM for all subtypes. PeIA[S9H] was applied at 10 μM for all subtypes and PeIA[S9H,V10A,E14N] was applied at 10 μM for $\alpha6/\alpha3\beta2\beta3$ and at 100 μM for $\alpha6/\alpha3\beta4$ nAChRs.

Data Analysis. The electrophysiology data were analyzed using GraphPad Prism software (GraphPad Software Inc., La Jolla, CA). Concentration-response curves for inhibition of I_{ACh} were generated by fitting the data to the Hill equation: % response = 100/{1 + ([toxin]/IC_{50})^{nH}}. Data for observed on rates (k_{obs}) were fit with a one-phase exponential equation and then analyzed by linear regression analysis to obtain an estimated value for k_{on}. Observed off-rate kinetics were assessed by fitting the I_{ACh} amplitudes with a one-phase exponential equation to obtain the plateau value of the I_{ACh}; observed values were then normalized to the plateau value and displayed as a percentage of the response to ACh.

Three-dimensional reconstructions of PeIA[S9H,V10A,E14N], MII, and PnIA were generated using PyMOL (PyMOL Molecular Graphics System, version 1.2r3pre; Schrödinger, LLC, New York, NY).

PeIA[S9H,V10A,E14N] was generated using the NMR structural coordinates of PeIA (Daly et al., 2011) as a template and the mutagenesis function of PyMOL. MII was also generated from NMR structural coordinates (Hill et al., 1998), and PnIA was generated from X-ray crystallography coordinates (Hu et al., 1996). Structures were generated without consideration of alternative rotameric positions of the side chains.

Results

Single Amino Acid Substitutions of PeIA Confer Increased Potency and Selectivity for the $\alpha6/\alpha3\beta2\beta3$ Subtype. α-Ctx PeIA was originally isolated from the fish-eating species *C. pergrandis* and at the time of its discovery was noted to be the first peptide ligand that potently blocked $\alpha9\alpha10$ but not $\alpha7$ nAChRs (McIntosh et al., 2005). However, PeIA also potently blocks several other nAChR subtypes including those that contain the $\alpha6$ subunit. PeIA shows a high degree of homology to other α-Ctxs that have four Cys residues that are connected by two disulfide bonds (Fig. 1A). Structure-function studies of α-Ctx MII indicated that residues of the second disulfide loop interact with residues of the $\alpha6$ nAChR subunit (McIntosh et al., 2004; Azam et al., 2008; Pucci et al., 2011). His residues in the 9th and 12th positions and Asn in the 14th position of MII are critical for conferring potency on $\alpha6/\alpha3\beta2\beta3$ nAChRs (McIntosh et al., 2004). For α-Ctx PnIA, Ala in the 10th position is critical for subtype selectivity and potency for $\beta2$-containing nAChRs (Hogg et al., 1999; Luo et al., 1999). Therefore, we reasoned that mutations in the homologous positions of PeIA not only might be permissive for retaining activity but also might confer beneficial changes in selectivity. We synthesized analogs that incorporated these nonconserved amino acids into the second disulfide loop of PeIA (Fig. 1A). These synthetic peptides were then evaluated for changes in potency and selectivity for the $\alpha6/\alpha3\beta2\beta3$ subtype using two-electrode voltage-clamp electrophysiology of *Xenopus* oocytes expressing cloned nAChRs. Substitution of Ser for His in the 9th position of PeIA increased the potency for inhibition of $\alpha6/\alpha3\beta2\beta3$ nAChRs by ~11-fold; increased potency was also

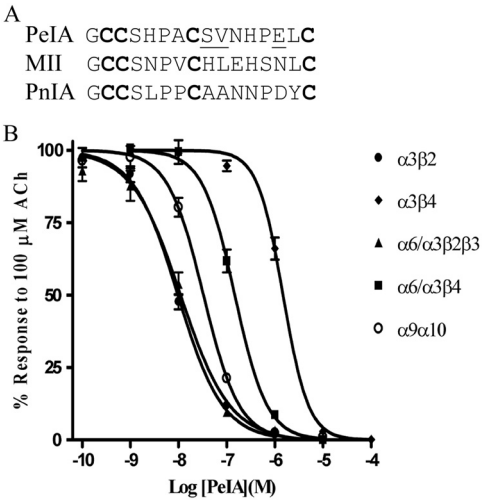

Fig. 1. Amino acid sequence comparison between α-Ctxs PeIA, MII, and PnIA. A, conserved cysteines are shown in bold; residues of PeIA that were selected for substitution with those of either MII or PnIA are shown underscored. B, concentration-response analysis of the activity of PeIA on *Xenopus* oocyte-expressed rat nAChRs. PeIA blocked I_{ACh} mediated by $\alpha3\beta2$, $\alpha3\beta4$, $\alpha6/\alpha3\beta2\beta3$, $\alpha6/\alpha3\beta4$, and $\alpha9\alpha10$ nAChRs with IC_{50} (95% confidence interval) values of 9.73 (8.11–11.7) nM, 1.5 (1.3–1.7) μM, 11.1 (8.17–15.0) nM, 148 (124–176) nM, and 33.0 (28.0–33.9) nM, respectively. Error bars denote the S.E.M. of the data from three to five oocytes for each determination.

observed on $\alpha3\beta2$, $\alpha6/\alpha3\beta4$, and $\alpha3\beta4$ nAChRs (Fig. 2A). In contrast, the S9H substitution resulted in an ~55-fold loss of potency on the $\alpha9\alpha10$ subtype (Fig. 2A). Next, we evaluated an Ala substitution for Val in the 10th position. Similar to the S9H analog, PeIA[V10A] showed increased activity on the $\alpha6/\alpha3\beta2\beta3$ nAChR, but, in contrast, showed an ~2-fold loss of activity on $\alpha6/\alpha3\beta4$ and $\alpha3\beta4$ nAChRs (Fig. 2B). The net result of this substitution was an analog with ~126-fold selectivity for $\alpha6/\alpha3\beta2\beta3$ versus the $\alpha6/\alpha3\beta4$ subtype. Finally, Asp was substituted for Glu14; although the activity was decreased for $\alpha6/\alpha3\beta2\beta3$ by ~2-fold, there was an ~3-fold loss of activity for $\alpha6/\alpha3\beta4$ and an ~15-fold loss for $\alpha3\beta2$ nAChRs (Fig. 2C). Table 1 summarizes the changes in IC_{50} values for inhibition of the four closely related $\alpha3$- and $\alpha6$-containing nAChR subtypes and compares the selectivity of each peptide for $\alpha6/\alpha3\beta2\beta3$ relative to that for the $\alpha6/\alpha3\beta4$ subtype.

We next examined the kinetics of block and unblock by PeIA and its singly substituted analogs. To obtain k_{obs}, the oocytes were perfused with a concentration of peptide within 10-fold of the peptides' respective IC_{50} values; 1-s pulses of ACh were applied once every minute until a steady-state block of the I_{ACh} was observed. To obtain k_{off}, a concentration of peptide that blocked >95% of the I_{ACh} (see *Materials and Methods*) was applied for 5 min in a static bath after which the peptide was washed out, and I_{ACh} was monitored for recovery. As shown in Fig. 3, the kinetics of block and unblock by the parent peptide PeIA were similar for all four of the nAChR subtypes tested. Block and recovery from block were rapid, and in most cases the $t_{1/2}$ times were <30 s. In contrast to the relatively rapid kinetics of PeIA, kinetics of the S9H analog were markedly slower (Fig. 3). Steady-state block by PeIA[S9H] of $\alpha6/\alpha3\beta2\beta3$ nAChRs using a 1 nM concentration required ~11 min ($t_{1/2}$ = 2.2 min). Recovery from block was also slow, and full recovery required ~30 min

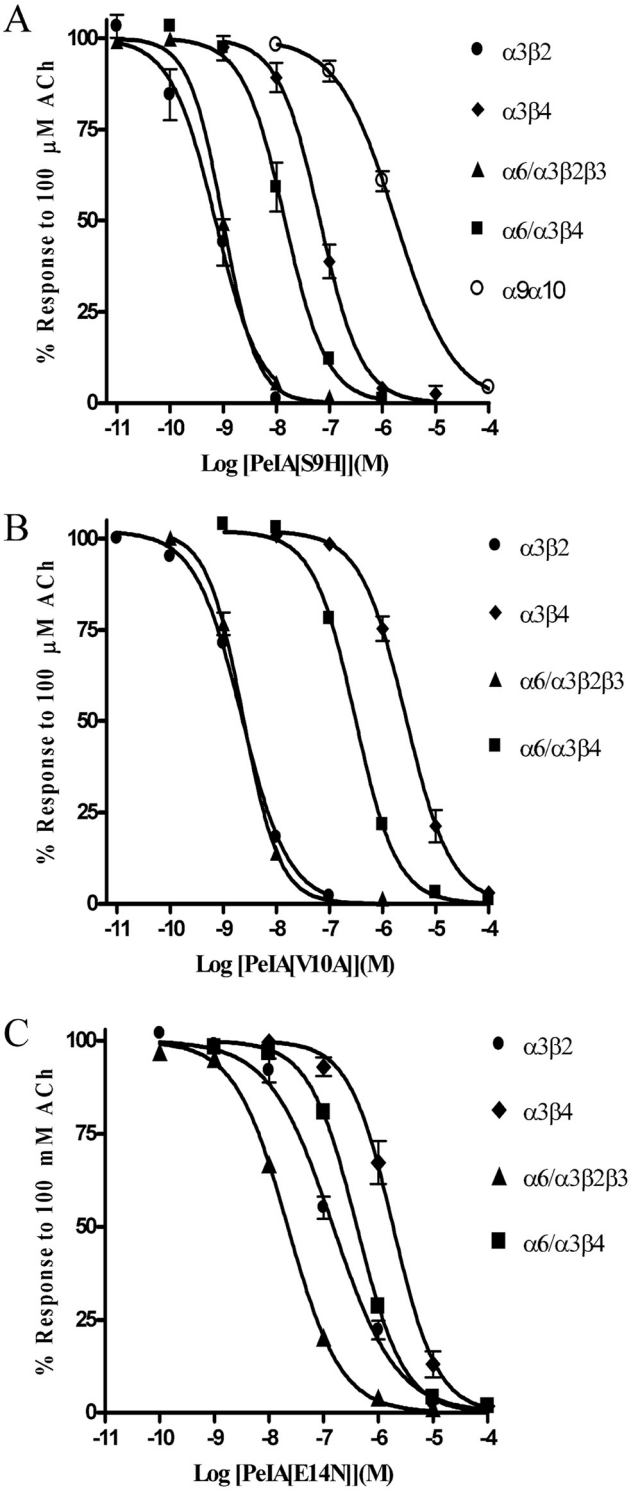

Fig. 2. Concentration-response analysis of the singly substituted PeIA analogs PeIA[S9H] (A), PeIA[V10A] (B), and PeIA[E14N] (C) on *Xenopus* oocyte-expressed rat α3β2, α3β4, α6/α3β2β3, α6/α3β4, and α9α10 nAChRs. The error bars for the data denote the S.E.M. from four to eight oocytes for each determination. IC_{50} values and confidence intervals are shown in Table 1.

($t_{1/2}$ = 6.2 min) of washout. The kinetics of the V10A analog were also slower than the kinetics of the native peptide but faster than those of PeIA[S9H] (Fig. 3). Kinetic analysis of block and recovery of block by PeIA and PeIA[V10A] of α6/α3β2β3 and α6/α3β4 yielded $t_{1/2}$ times of <60 s, so an accurate comparison of the change in affinity between PeIA[V10A] and the native peptide could not be made. However, the ~2-fold increase in the IC_{50} value for PeIA[V10A] for inhibition of α6/α3β4 nAChRs implies that either k_{on} is slower or k_{off} is faster and contributes to the ~126-fold separation between the IC_{50} values for inhibition of α6/α3β2β3 versus α6/α3β4 nAChRs. Likewise, the kinetics of PeIA[E14N] were too fast ($t_{1/2}$ times of <60 s for all subtypes) to permit accurate measurement of k_{obs} and k_{off} under the conditions used in this study. Table 2 summarizes the kinetic data for block and recovery from block by PeIA[S9H] and PeIA[V10A] for the four nAChR subtypes that were examined.

Combined Double and Triple Amino Acid Substitutions Confer Further Increases in Potency and Selectivity for α6/α3β2β3 nAChRs. All three of the single amino acid substitutions (Fig. 2) produced improvements in either potency or selectivity for the α6/α3β2β3 subtype. Therefore, we combined the S9H substitution with either the V10A or the E14N substitution to produce second-generation analogs. As shown in Fig. 4, PeIA[S9H,V10A] retained the high potency of the singly substituted S9H analog as well as the selectivity of the V10A analog. The IC_{50} value for block of α6/α3β2β3 was ~2-fold lower than that of PeIA[S9H], whereas an ~4-fold increase in the IC_{50} value was observed for α6/α3β4 nAChRs. Likewise, the selectivity ratio (~126-fold) of PeIA[V10A] for block of α6/α3β2β3 versus α6/α3β4 was also retained. Of interest, PeIA[S9H,E14N] retained high potency for the α6/α3β2β3 nAChR (IC_{50} = 753 pM), which is ~39-fold more potent than block of α6/α3β4 nAChRs. Finally, we combined all three amino acid substitutions to generate PeIA[S9H,V10A,E14N]. This triply substituted analog was ~290-fold more potent at blocking the α6/α3β2β3 subtype than the α6/α3β4 subtype (Fig. 5A). As discussed above, oocytes injected with nonchimeric α6 in combination with β2 and β3 constructs fail to produce functional responses. However, injection of α6 with β4 does yield functional responses albeit relatively small in amplitude. The α6β4-mediated currents evoked by 100 μM ACh were on average 10.2 ± 1.1 nA (n = 5) and were blocked by PeIA[S9H,V10A,E14N] with an IC_{50} (95% confidence interval) value of 66.0 (51.5–84.7) nM, similar to the 65.4 (43.4–98.6) nM value obtained using chimeric α6/α3β4 nAChRs (Fig. 5A). We also tested this triply substituted PeIA analog on cloned mouse and cloned human α6-containing nAChRs. The IC_{50} values obtained for mouse α6/α3β2β3 and α6/α3β4 were also similar to those obtained using the rat counterparts (Fig. 5A). Likewise, the activity was similar when tested on concatameric human α6β2α4β2β3 (Fig. 5A) and chimeric rat α6/α4β2β3 nAChRs (Supplemental Fig. 1). PeIA[S9H,V10A,E14N] also inhibited rat α3β2 nAChRs but was much less potent when tested on other rat subtypes including α3β4, α4β2, α4β4, α7, and α9α10 (Fig. 5B). Tables 3 and 4 summarize the activity of the doubly and triply substituted analogs on the nAChRs tested.

PeIA[S9H,V10A,E14N] Potently and Selectively Blocks the α6/α3β2β3 versus the α6/α3β4 Subtype. To more fully examine the ability of PeIA[S9H,V10A,E14N] to discriminate between the α6/α3β2β3 and the α6/α3β4 subtypes, we conducted an in depth characterization of the pharmacological properties of the peptide. First, we deter-

TABLE 1

IC_{50} values for inhibition of rat nAChRs expressed in *Xenopus* oocytes

Numbers in parentheses are 95% confidence intervals.

	α3β2	α6/α3β2β3	α3β4	α6/α3β4	α6/α3β4/α6/α3β2β3 Ratio
PeIA	9.7 (8.1–11.7) nM	11.1 (8.2–15.0) nM	1.5 (1.3–1.7) μM	147 (124–176) nM	13
PeIA[S9H]	713 (480–1060) pM	991 (932–1054) pM	66 (52–84) nM	14.5 (11.3–18.6) nM	15
PeIA[V10A]	2.2 (2.0–2.5) nM	2.4 (2.1–2.7) nM	2.7 (2.2–3.3) μM	302 (278–330) nM	126
PeIA[E14N]	149 (122–182) nM	22.0 (19.6–24.6) nM	1.9 (1.5–2.4) μM	406 (385–427) nM	18

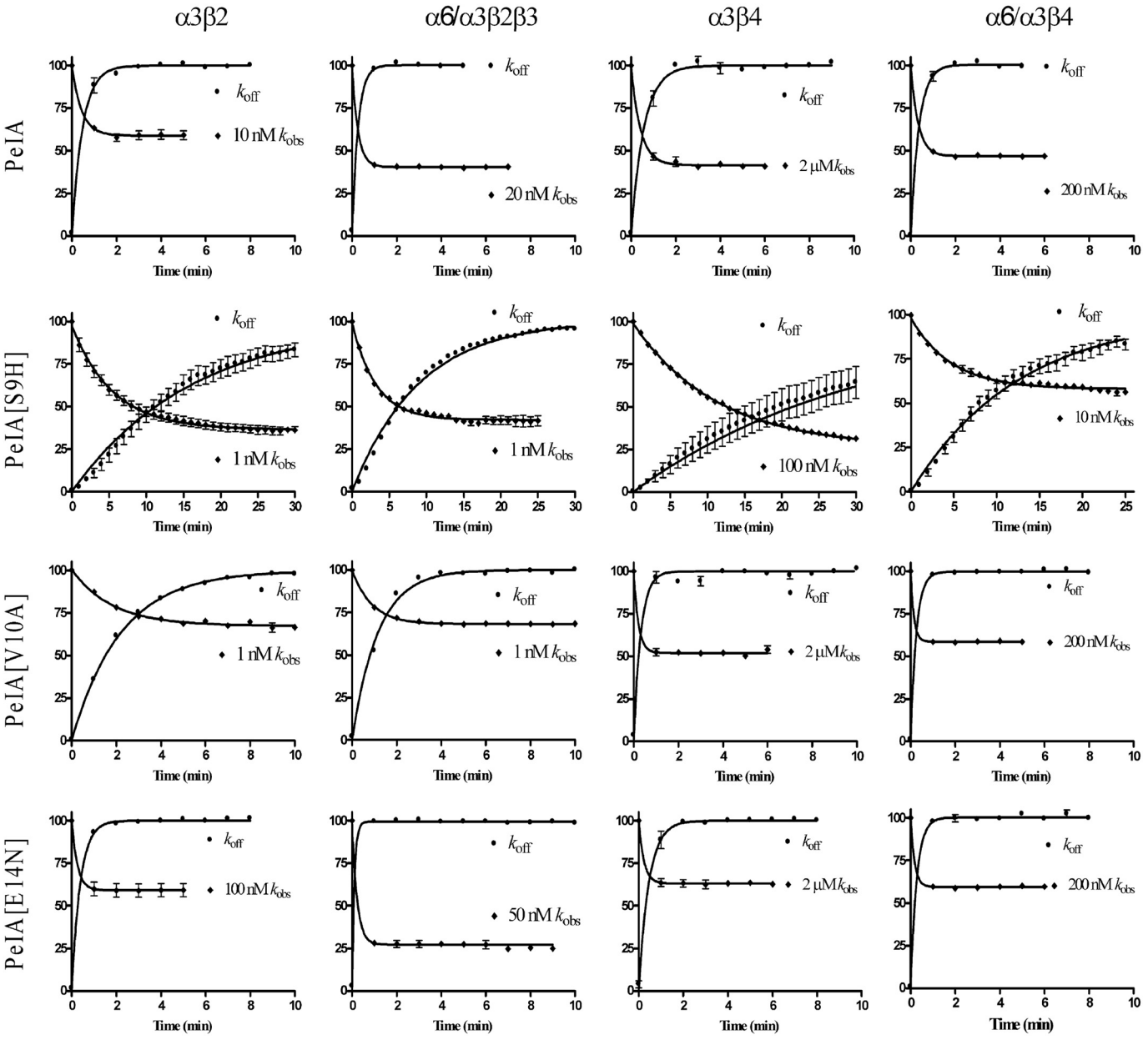

Fig. 3. Kinetic analysis of the activity of PeIA and single substituted analogs on *Xenopus* oocyte-expressed rat α3β2, α3β4, α6/α3β2β3, and α6/α3β4 nAChRs. The toxins were applied as described under *Materials and Methods*, and the data were fit to a single exponential equation. The error bars denote the S.E.M. of the data from three to nine oocytes for each determination. Note the different time scale used for PeIA[S9H]. See Table 2 for a summary of the values obtained.

mined k_{on} by perfusing oocytes expressing α6/α3β2β3 with five different concentrations of PeIA[S9H,V10A,E14N] from 100 pM to 5 nM until steady-state block was achieved (Fig. 6A). The data were analyzed using a one-phase exponential to obtain the k_{obs} for each of the concentrations tested, and the data are plotted as a function of concentration. This analysis yielded a slope (k_{on}) of 0.228 ± 0.019 min^{-1} M^{-9} (Fig. 6B). A k_{off} value of 0.096 ± 0.001 min^{-1} was obtained by applying a high concentration of peptide to the oocyte in a 5-min static bath (Fig. 6C). Because the dissociation constant is a ratio of k_{off} to k_{on}, an estimated K_i value of 423 pM was obtained. Applying this same

TABLE 2
Kinetic analysis of block and recovery from block by PeIA[S9H] and PeIA[V10A]
Data are means ± S.E.M. from three to nine oocytes. Numbers in parentheses are 95% confidence intervals.

	k_{off}	k_{obs}	k_{on}	K_i
	min^{-1}	min^{-1}	$min^{-1}\ M^{-1}$	M^{-9}
α3β2				
PeIA[S9H]	0.062 ± 0.001 (0.059–0.064)	0.18 ± 0.01 (0.161–0.204)	0.118 ± 0.01× 10^{9a}	0.525[b]
PeIA[V10A]	0.456 ± 0.008 (0.440–0.472)	0.55 ± 0.04 (0.46–0.62)	0.94 ± 0.04× 10^{8a}	4.85[b]
α6/α3β2β3				
PeIA[S9H]	0.11 ± 0.01 (0.10–0.12)	0.31 ± 0.01 (0.29–0.34)	0.200 ± 0.01× 10^{9a}	0.550[b]
α3β4				
PeIA[S9H]	0.032 ± 0.001 (0.030–0.034)	0.088 ± 0.002 (0.084–0.093)	0.56 ± 0.002×10^{6a}	57[b]
α6/α3β4				
PeIA[S9H]	0.078 ± 0.001 (0.075–0.081)	0.21 ± 0.01 (0.184–0.240)	0.132 ± 0.01× 10^{8a}	5.9[a]

[a] Calculated from $k_{obs} = k_{on}$ [toxin] + k_{off}.
[b] Calculated from $K_i = k_{off}/k_{on}$.

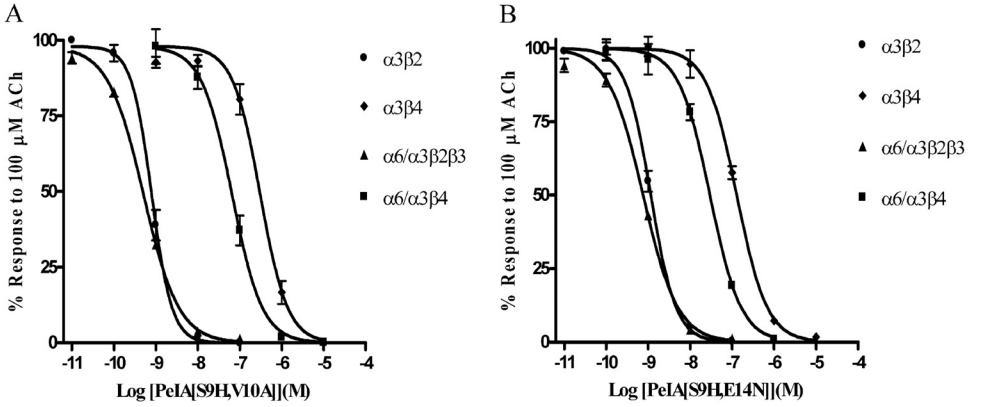

Fig. 4. Concentration-response analysis of the doubly substituted PeIA analogs PeIA[S9H,V10A] (A) and PeIA[S9H,E14N] (B) on *Xenopus* oocyte-expressed rat α3β2, α3β4, α6/α3β2β3, and α6/α3β4 nAChRs. The error bars for the data denote the S.E.M. from three to five oocytes for each determination. For a summary of the IC_{50} values and confidence intervals see Table 3.

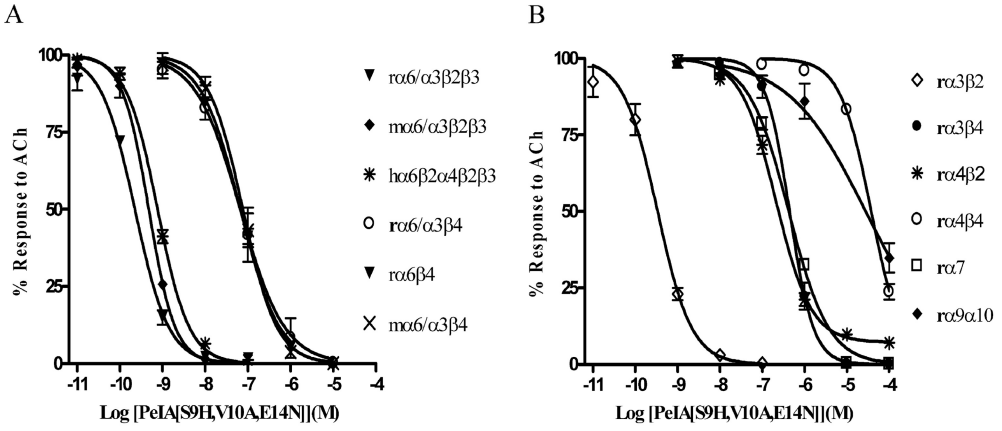

Fig. 5. Concentration-response analysis of the activity of PeIA[S9H,V10A,E14N] on *Xenopus* oocyte-expressed nAChR subtypes. A, inhibition curves for rα6/α3β2β3, mα6/α3β2β3, hα6β2α4β2β3, rα6/α3β4, rα6β4, and mα6/α3β4 nAChRs. B, inhibition curves for rα3β2, rα3β4, rα4β2, rα4β4, rα7, and rα9β10 nAChRs. The error bars for the data denote the S.E.M. from four to five oocytes for each determination; r, rat; m, mouse; h, human. For a summary of the IC_{50} values and confidence intervals see Table 4.

TABLE 3
IC_{50} values for inhibition of rat nAChRs by doubly substituted analogs of PeIA
Numbers in parentheses are 95% confidence intervals.

	α3β2	α6/α3β2β3	α3β4	α6/α3β4	Ratio of α6/α3β4 to α6/α3β2β3
PeIA[S9H,V10A]	793 (675–932) pM	506 (455–564) pM	307 (240–394) nM	65.1 (50.0–84.8) nM	129
PeIA[S9H,E14N]	1.15 (1.02–1.09) nM	753 (656–864) pM	128 (109–151) nM	29.5 (24.4–34.6) nM	39

methodology to oocytes expressing α6/α3β4 nAChRs over a concentration range of 10 to 500 nM yielded a k_{on} of 0.699 ± 0.023 $min^{-1}\ M^{-7}$ (Fig. 6, D and E) and an observed k_{off} value of 0.626 ± 0.02 min^{-1}. The estimated K_i for α6/α3β4 was ~90 nM, a value >200-fold higher than that determined for α6/α3β2β3 nAChRs. Thus, from a functional standpoint, a concentration of 5 nM would be expected to produce near complete inhibition of α6/α3β2β3 nAChRs but show little block of the α6/α3β4 subtype. Indeed, in the presence of 5 nM PeIA[S9H,V10A,E14N], the I_{ACh} values mediated by α6/α3β2β3 nAChRs were only 3.0 ± 0.2% of the control I_{ACh}, whereas those mediated by α6/α3β4 nAChRs were on average 94.0 ± 4% of control responses (Fig. 7, A–C).

TABLE 4
Activity of PeIA[S9H,V10A,E14N] on nAChRs expressed in *Xenopus* oocytes

nAChR Subtype	IC_{50}	95% Confidence Interval	IC_{50} ratios (Compared with Rat $\alpha6/\alpha3\beta2\beta3$)
r$\alpha3\beta2$	335 pM	264–423	1.5
r$\alpha3\beta4$	441 nM	370–527	1970
r$\alpha4\beta2$	209 nM	169–258	937
r$\alpha4\beta4$	37.6 μM	32.9–43.0	>10,000
r$\alpha6/\alpha3\beta2\beta3$	223 pM	186–266	1
m$\alpha6/\alpha3\beta2\beta3$	470 pM	393–652	2.0
h$\alpha6\beta2\alpha4\beta2\beta3$	759 pM	685–842	3.4
r$\alpha6\beta4$	66.0 nM	51.4–84.7	296
r$\alpha6/\alpha3\beta4$	65.4 nM	43.4–98.6	293
m$\alpha6/\alpha3\beta4$	75.6 nM	61.1–96.3	339
r$\alpha7$	421 nM	356–498	1880
r$\alpha9\alpha10$	27.8 μM	15.5–50.0	>10,000

r, rat; m, mouse; h, human concatamer.

Discussion

α-Ctx PeIA was originally described as the first ligand that could discriminate between $\alpha9\alpha10$ and $\alpha7$ nAChRs (McIntosh et al., 2005). It is noteworthy that although PeIA shares an activity profile similar to that of other α-Ctxs that target $\alpha3\beta2$ and $\alpha6/\alpha3\beta2\beta3$ nAChRs, specifically MII (Cartier et al., 1996; McIntosh et al., 2004) and PnIA (Hogg et al., 1999; Luo et al., 1999; Hone et al., 2012), it is only 42% similar to these peptides in noncysteine amino acid homology (Fig. 1A). Despite their sequence differences, molecular modeling and solution NMR studies predict that PeIA, MII, and PnIA all share a similar three-dimensional backbone structure and occupy the acetylcholine binding pocket in approximately the same orientation (Rogers et al., 1999; Daly et al., 2011; Pucci et al., 2011). These differences and similarities suggest that specific residues of the peptides might be critical for binding to $\alpha6\beta2$-containing nAChRs. Thus, one aim of this study was to gain mechanistic insight into the binding of ligands with $\alpha6\beta2$-containing nAChRs. To this end, we substituted specific amino acids of PeIA with those of MII and PnIA that are known to be critical for activity and evaluated the substituted analogs for changes in potency and selectivity for the $\alpha6/\alpha3\beta2\beta3$ subtype.

Native PeIA shows a modest degree of separation (~13-fold) between the IC_{50} values for $\alpha6/\alpha3\beta2\beta3$ and the $\alpha6/\alpha3\beta4$ subtypes. Thus, coupled with the known activity on

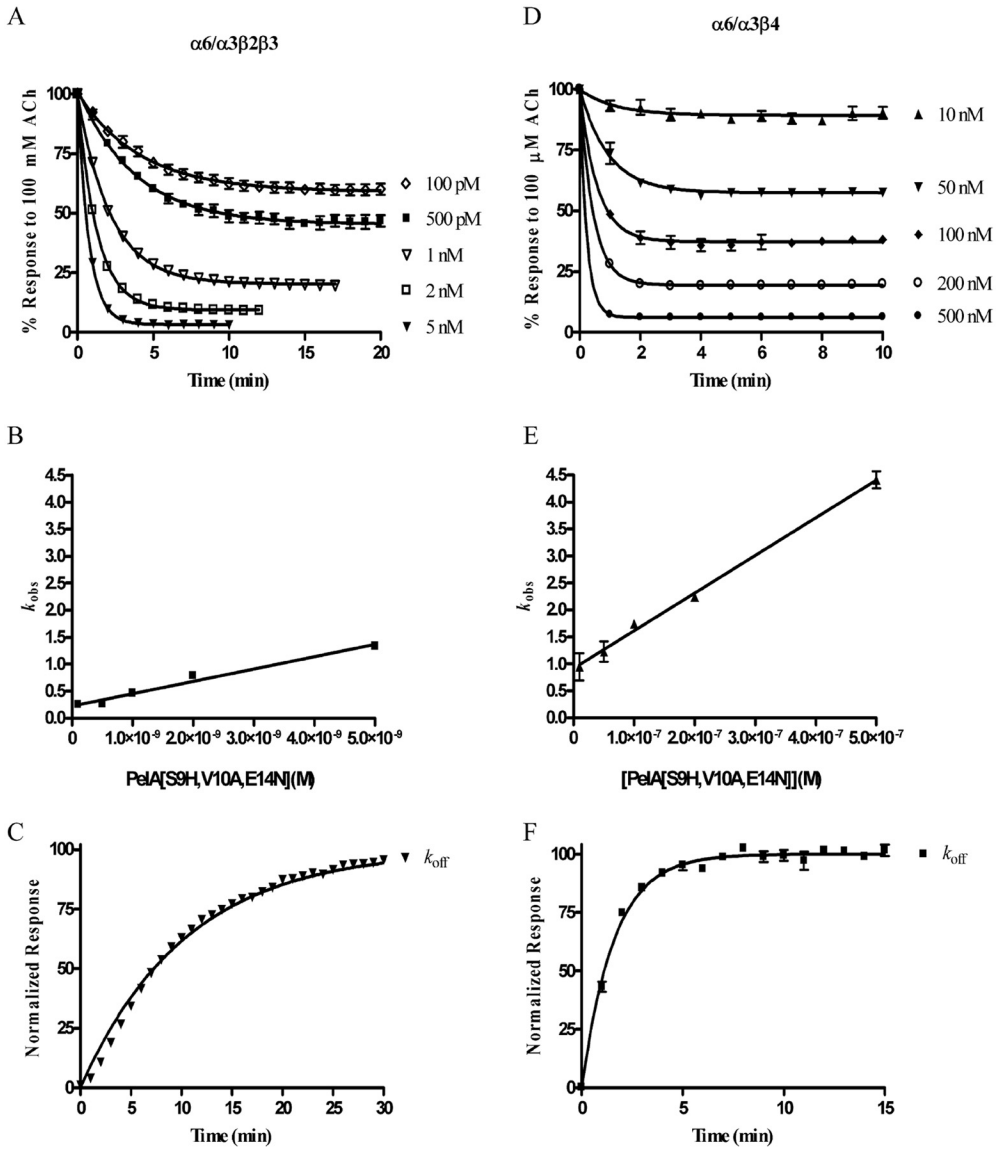

Fig. 6. Comparison of PeIA[S9H,V10A,E14N] kinetics on rat $\alpha6/\alpha3\beta2\beta3$ versus $\alpha6/\alpha3\beta4$ nAChRs expressed in *Xenopus* oocytes. A, k_{obs} was determined for five concentrations of PeIA[S9H,V10A,E14N] from 100 pM to 5 nM by perfusing the oocytes with the toxin until a steady-state level of block was achieved. B, the data were fit to an exponential equation, and the observed rates are plotted as a function of the PeIA[S9H,V10A,E14N] concentration to obtain k_{on}. C, to obtain k_{off}, a high concentration of toxin was applied in a static bath for 5 min after which the perfusion was resumed, and the I_{ACh} was monitored for recovery (see *Materials and Methods* for the concentrations used). The same analysis was performed for $\alpha6/\alpha3\beta4$ nAChRs (D–F). The error bars in A to C denote the S.E.M. from four individual determinations and from five in D to F.

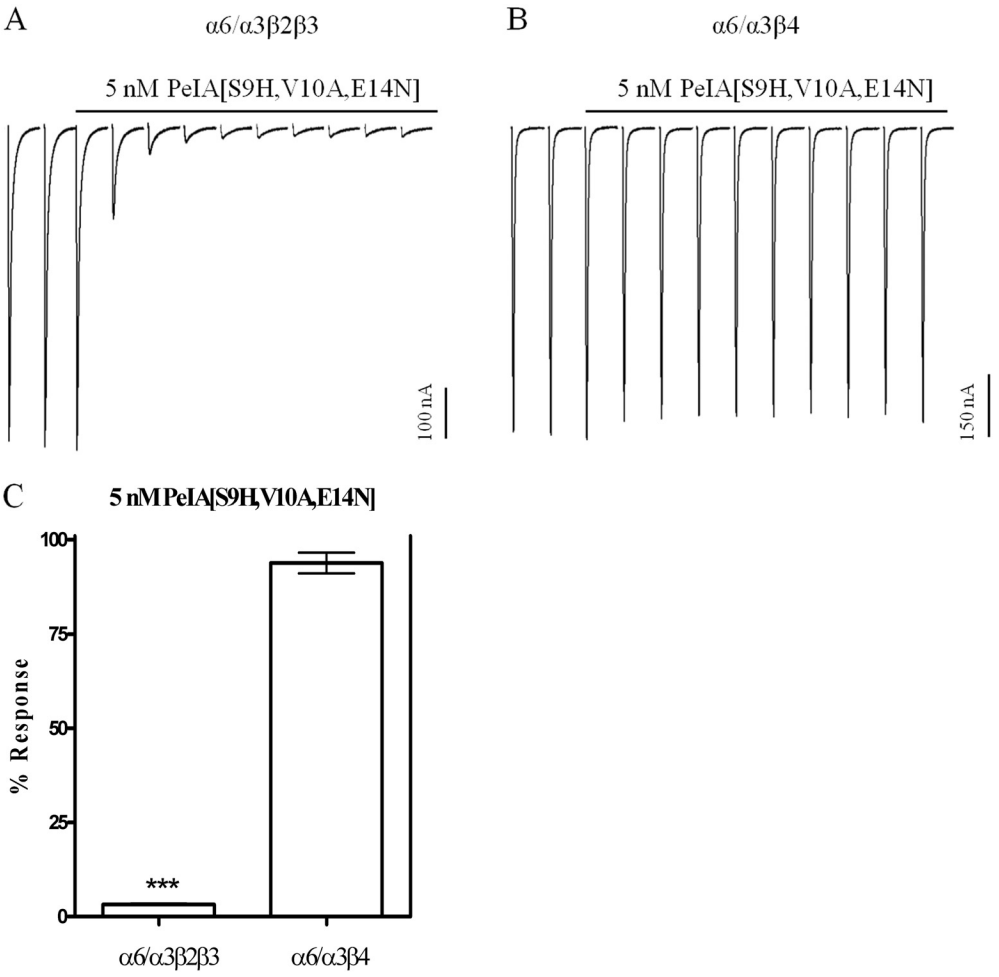

Fig. 7. Block of α6/α3β2β3 and α6/α3β4 nAChRs by PeIA[S9H,V10A,E14N]. Oocytes expressing α6/α3β2β3 (A) and α6/α3β4 (B) nAChRs were continuously perfused with 5 nM PeIA[S9H,V10A,E14N] until a steady-state level of block was achieved; the percentage response was then quantified for comparison (C). The error bars in C denote the S.E.M. from four oocytes expressing the α6/α3β2β3 subtype and from six expressing the α6/α3β4 subtype. Significance was determined by a *t* test and compared with a theoretical response mean of 100%. ***, $p < 0.001$.

other nAChR subtypes, PeIA is a nonselective antagonist of the five nAChR subtypes listed in Fig. 1B. However, structure-function studies of α-Ctxs MII (McIntosh et al., 2004), PnIA (Hogg et al., 1999; Luo et al., 1999), and BuIA (Azam et al., 2010) suggested that PeIA would be a promising platform from which to develop α6β2-selective ligands. These studies demonstrated that specific amino acids of MII confer high potency for the α6/α3β2β3 subtype and that the 10th position in PnIA is critical for subtype selectivity and provided a rational strategy for engineering α6/α3β2β3 subtype-selective ligands using PeIA as a template.

In this report, we describe the synthesis and characterization of a potent antagonist of α6/α3β2β3 nAChRs achieved by substituting critical amino acids in the second loop of PeIA that increased potency and selectivity for α6/α3β2β3 versus α6/α3β4 nAChRs. These amino acids included Ser9, Val10, and Glu14 and were substituted with His, Ala, and Asn, respectively. When tested on *Xenopus* oocytes that expressed rat α6/α3β2β3 or α6/α3β4 nAChRs, the S9H substitution had the largest impact on potency and shifted the IC_{50} value for inhibition of α6/α3β2β3 nAChRs by ~11-fold, whereas the V10A substitution had the largest effect on selectivity and conferred an ~10-fold increase in separation between the two subtypes (Fig. 2, A and B) over the native peptide. An additional ~5-fold increase in selectivity for α6/α3β2β3 versus α6/α3β4 nAChRs over the native peptide was observed with the Glu for Asn substitution in the 14th position (Fig. 2C). The V10A and E14N substitutions were combined in pairwise fashion with S9H with the expectation that double substitutions would retain the effects observed with each respective single substitution. Indeed, both PeIA[S9H,V10A] and PeIA[S9H,E14N] retained the selectivity of PeIA[V10A] and PeIA[E14N], and, interestingly, both doubly substituted analogs were even more potent than PeIA[S9H] (Figs. 2A and 4, A and B). Finally, PeIA[S9H,V10A,E14N] was synthesized, combining all three single substitutions to generate a ligand that was ~50-fold more potent than native PeIA for inhibition of α6/α3β2β3 nAChRs (Figs. 1B and 5A), and produced an ~1800-fold improvement in selectivity for α6/α3β2β3 versus α3β4 and an ~1700-fold improvement versus α7 nAChRs (IC_{50} = 1.8 μM) (McIntosh et al., 2005) over native PeIA (Fig. 5, A and B). Of most importance, an ~280-fold improvement was observed for α6/α3β2β3 versus the α6/α3β4 subtype (Fig. 5A).

The kinetics of block and recovery from block were assessed on α6/α3β2β3 nAChRs and compared with those obtained for the α6/α3β4 subtype (Fig. 6, A–F). These studies yielded a K_i value for α6/α3β2β3 (423 pM) that was >200-fold lower than that obtained for α6/α3β4 (~90 nM) nAChRs (Fig. 6, A–F). Thus, at reasonable concentrations (5–10 times the K_i) for inhibition of α6/α3β2β3 nAChRs, little inhibition of α6/α3β4 nAChRs would be expected (Fig. 7). PeIA[S9H,V10A,E14N] was also tested on six other non-α6-containing nAChR subtypes and

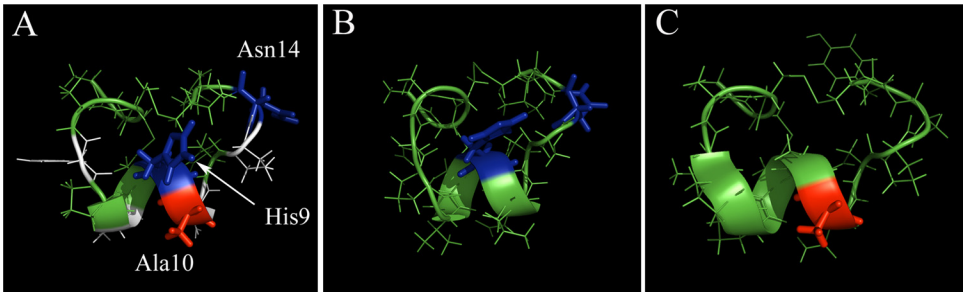

Fig. 8. Comparison of the three-dimensional structures of PeIA[S9H,V10A,E14N], MII, and PnIA. A, α-Ctx PeIA[S9H,V10A,E14N] with residues substituted from MII shown in blue (His9) and (Asn14) and from PnIA shown in red (Ala10). Residues shown in white are nonhomologous with MII. B, α-Ctx MII with His9 and Asn14 shown in blue. C, α-Ctx PnIA with Ala10 shown in red. Images were generated using PyMOL as described under *Materials and Methods*.

although inhibition of the two major central nervous system subtypes, $\alpha4\beta2$ and $\alpha7$, was observed, the IC_{50} values were ~930- and ~1800-fold higher, respectively, than the IC_{50} value for $\alpha6/\alpha3\beta2\beta3$ nAChRs (Fig. 5, A and B). However, the peptide does retain high potency for the $\alpha3\beta2$ subtype and cannot be used to discriminate between this subtype and $\alpha6/\alpha3\beta2\beta3$ nAChRs.

An analog of α-Ctx MII, MII[E11A], also shows some selectivity (40-fold) for $\alpha6/\alpha3\beta2\beta3$ versus $\alpha6/\alpha3\beta4$ nAChRs (McIntosh et al., 2004). PnIA also preferentially targets $\alpha6/\alpha3\beta2\beta3$ nAChRs but with ~50-fold lower potency (Hone et al., 2012) than PeIA[S9H,V10A,E14N] and with significantly overlapping activity on the $\alpha7$ subtype (Luo et al., 1999). We note that the sequence of PeIA[S9H,V10A,E14N] is 75% identical to that of MII[E11A] in terms of noncysteine amino acids, differing in the second loops by residues in the 10th, 11th, and 13th positions yet the PeIA analog is ~7-fold more selective for $\alpha6/\alpha3\beta2\beta3$ versus $\alpha6/\alpha3\beta4$ nAChRs than MII[E11A]. Of interest, when we substituted Ala for Asn in the 11th position to make PeIA more MII[E11A]-like, an ~5-fold loss of potency was observed (data not shown). In addition, substitution of Asn with that of native MII (Glu) in the 11th position of PeIA[S9H,V10A] also resulted in a loss in potency of ~12-fold (data not shown). The $\alpha6$ ligand-binding pocket contains three Glu and one Asp residues that are thought to interact with residue 11 of MII and its analogs (Azam et al., 2008; Pucci et al., 2011). Thus, the introduction of the negatively charged amino acid Glu may produce a repulsive electrostatic interaction between Glu and the highly negatively charged $\alpha6$ subunit interface. This would be consistent with the results of others who found that replacement of Glu with a positively charged Arg in the 11th position increased the potency of MII (Pucci et al., 2011). However, this mechanism would not account for the increased potency observed with MII[E11A] because Ala is uncharged. Thus, although the three-dimensional backbone structures of PeIA[S9H,V10A,E14N], MII, and PnIA are predicted to be similar (Fig. 8), differences in amino acid side chains are critical for activity on the $\alpha6\beta2$-containing nAChR. Specific amino acid side chains may directly interact with residues of the receptor or influence different conformations of neighboring amino acid side chains. These possibilities together with our results with PeIA suggest a more complex interaction between α-Ctxs and the $\alpha6\beta2$ binding site. It would therefore be highly informative to conduct a positional scanning study on PeIA coupled with site-directed mutagenesis of the $\alpha6$ subunit to gain further mechanistic insights into the interaction between ligands and the $\alpha6\beta2$-containing nAChR.

The $\alpha6\beta2^*$ subtype has received considerable attention recently, and consequently significant efforts have been undertaken to develop highly specific ligands to study this receptor subtype in areas where multiple nAChR subtypes are potentially expressed (Letchworth and Whiteaker, 2011; Pivavarchyk et al., 2011; Pucci et al., 2011). Significant heterogeneity of nAChR expression typifies many neuronal populations in the nervous system, and such is the case in striatum where the predominant subtypes are $\alpha6\beta2^*$ and $\alpha4\beta2^*$ (Grady et al., 2007; Perez et al., 2008) and in the ventral tegmental area where the predominant subtypes are $\alpha6\beta2^*$, $\alpha4\beta2^*$, $\alpha7$, and a currently uncharacterized $\beta4$-containing nAChR (Wooltorton et al., 2003; Jones and Wonnacott, 2004; Wu et al., 2004; Yang et al., 2009). In certain regions of the primate brain such as the cerebellum, substantial overlap of $\alpha6$, $\beta2$, and $\beta4$ subunit mRNAs have been found (Quik et al., 2000). Furthermore, $\alpha6\beta4^*$ nAChRs have recently been identified in human adrenal chromaffin cells and characterized using analogs of MII (Pérez-Alvarez et al., 2012). However, the analogs used in this study also potently block $\alpha6/\alpha3\beta2\beta3$, but not $\alpha3\beta2$ nAChRs, and, therefore, the presence of $\alpha6\beta2^*$ nAChRs cannot be ruled out. The $\alpha6\beta4^*$ subtype has also been recently identified in a population of rat dorsal root ganglion neurons that also express $\beta2$-containing nAChRs of the $\alpha6\beta2^*$ and/or the $\alpha3\beta2^*$ subtypes (Hone et al., 2012). Whereas PeIA[S9H,V10A,E14N] does not distinguish between these two subtypes, MII[H9A,L15] does (McIntosh et al., 2004). Thus, an approach using the selectivity profiles of both toxins may be useful for identifying the $\beta2$-containing nAChRs in these neurons. The fact that PeIA[S9H,V10A,E14N] blocks rat, mouse, and human $\alpha6\beta2$-containing nAChRs with similar potencies while maintaining selectivity for $\alpha6\beta2$-containing versus $\alpha6\beta4$-containing nAChRs will allow the toxin to be used across species and thus should prove particularly useful for distinguishing $\alpha6\beta2^*$ from $\alpha6\beta4^*$ nAChRs in tissues in which these receptors are potentially coexpressed. Finally, it is noteworthy that PeIA[S9H,V10A,E14N] is 1300-fold more potent at blocking $\alpha3\beta2$ than $\alpha3\beta4$ nAChRs. This exquisite selectivity for $\alpha3\beta2$ nAChRs may be useful for distinguishing between these two subtypes in neurons such as those found in intracardiac ganglia (Bibevski et al., 2000) and superior cervical ganglia (Mao et al., 2006; David et al.,

2010), which predominantly express a mixed population of α3-containing nAChRs.

Acknowledgments

We thank Bob Shackman at the DNA/Peptide Synthesis core facility at the University of Utah for assistance with peptide synthesis, Miguel Ruiz, Phuong Tran, and Melissa McIntyre for assistance with peptide folding, and William Lowe at the Salk Institute for Biological Studies for performing the matrix-assisted laser desorption ionization mass spectrometry.

Authorship Contributions

Participated in research design: Hone and McIntosh.
Conducted experiments: Hone, Scadden, Gajewiak, and Christensen.
Contributed new reagents or analytic tools: Lindstrom.
Performed data analysis: Hone and Scadden.
Wrote or contributed to the writing of the manuscript: Hone, Gajewiak, and McIntosh.

References

Armishaw CJ (2010) Synthetic α-conotoxin mutants as probes for studying nicotinic acetylcholine receptors and in the development of novel drug leads. *Toxins (Basel)* **2:**1471–1499.
Azam L, Maskos U, Changeux JP, Dowell CD, Christensen S, De Biasi M, and McIntosh JM (2010) α-Conotoxin BuIA[T5A;P6O]: a novel ligand that discriminates between α6β4 and α6β2 nicotinic acetylcholine receptors and blocks nicotine-stimulated norepinephrine release. *FASEB J* **24:**5113–5123.
Azam L and McIntosh JM (2006) Characterization of nicotinic acetylcholine receptors that modulate nicotine-evoked [^{3}H]norepinephrine release from mouse hippocampal synaptosomes. *Mol Pharmacol* **70:**967–976.
Azam L and McIntosh JM (2009) α-Conotoxins as pharmacological probes of nicotinic acetylcholine receptors. *Acta Pharmacol Sin* **30:**771–783.
Azam L, Yoshikami D, and McIntosh JM (2008) Amino acid residues that confer high selectivity of the α6 nicotinic acetylcholine receptor subunit to α-conotoxin MII[S4A,E11A,L15A]. *J Biol Chem* **283:**11625–11632.
Bibevski S, Zhou Y, McIntosh JM, Zigmond RE, and Dunlap ME(2000) Functional nicotinic acetylcholine receptors that mediate ganglionic transmission in cardiac parasympathetic neurons. *J Neurosci* **20:**5076–5082.
Bordia T, Grady SR, McIntosh JM, and Quik M (2007) Nigrostriatal damage preferentially decreases a subpopulation of α6β2* nAChRs in mouse, monkey, and Parkinson's disease striatum. *Mol Pharmacol* **72:**52–61.
Brunzell DH, Boschen KE, Hendrick ES, Beardsley PM, and McIntosh JM (2010) α-Conotoxin MII-sensitive nicotinic acetylcholine receptors in the nucleus accumbens shell regulate progressive ratio responding maintained by nicotine. *Neuropsychopharmacology* **35:**665–673.
Capelli AM, Castelletti L, Chen YH, Van der Keyl H, Pucci L, Oliosi B, Salvagno C, Bertani B, Gotti C, Powell A, et al. (2011) Stable expression and functional characterization of a human nicotinic acetylcholine receptor with α6β2 properties: discovery of selective antagonists. *Br J Pharmacol* **163:**313–329.
Cartier GE, Yoshikami D, Gray WR, Luo S, Olivera BM, and McIntosh JM (1996) A new α-conotoxin which targets α3β2 nicotinic acetylcholine receptors. *J Biol Chem* **271:**7522–7528.
Daly NL, Callaghan B, Clark RJ, Nevin ST, Adams DJ, and Craik DJ (2011) Structure and activity of α-conotoxin PeIA at nicotinic acetylcholine receptor subtypes and $GABA_B$ receptor-coupled N-type calcium channels. *J Biol Chem* **286:**10233–10237.
Dash B, Bhakta M, Chang Y, and Lukas RJ (2011) Identification of N-terminal extracellular domain determinants in nicotinic acetylcholine receptor (nAChR) α6 subunits that influence effects of wild-type or mutant β3 subunits on function of α6β2*- or α6β4*-nAChR. *J Biol Chem* **286:**37976–37989.
David R, Ciuraszkiewicz A, Simeone X, Orr-Urtreger A, Papke RL, McIntosh JM, Huck S, and Scholze P (2010) Biochemical and functional properties of distinct nicotinic acetylcholine receptors in the superior cervical ganglion of mice with targeted deletions of nAChR subunit genes. *Eur J Neurosci* **31:**978–993.
Dowell C, Olivera BM, Garrett JE, Staheli ST, Watkins M, Kuryatov A, Yoshikami D, Lindstrom JM, and McIntosh JM (2003) α-Conotoxin PIA is selective for α6 subunit-containing nicotinic acetylcholine receptors. *J Neurosci* **23:**8445–8452.
Exley R, Maubourguet N, David V, Eddine R, Evrard A, Pons S, Marti F, Threlfell S, Cazala P, McIntosh JM, et al. (2011) Distinct contributions of nicotinic acetylcholine receptor subunit α4 and subunit α6 to the reinforcing effects of nicotine. *Proc Natl Acad Sci USA* **108:**7577–7582.
Gotti C, Guiducci S, Tedesco V, Corbioli S, Zanetti L, Moretti M, Zanardi A, Rimondini R, Mugnaini M, Clementi F, et al. (2010) Nicotinic acetylcholine receptors in the mesolimbic pathway: primary role of ventral tegmental area α6β2* receptors in mediating systemic nicotine effects on dopamine release, locomotion, and reinforcement. *J Neurosci* **30:**5311–5325.
Grady SR, Salminen O, Laverty DC, Whiteaker P, McIntosh JM, Collins AC, and Marks MJ (2007) The subtypes of nicotinic acetylcholine receptors on dopaminergic terminals of mouse striatum. *Biochem Pharmacol* **74:**1235–1246.
Hill JM, Oomen CJ, Miranda LP, Bingham JP, Alewood PF, and Craik DJ (1998) Three-dimensional solution structure of α-conotoxin MII by NMR spectroscopy: effects of solution environment on helicity. *Biochemistry* **37:**15621–15630.
Hogg RC, Miranda LP, Craik DJ, Lewis RJ, Alewood PF, and Adams DJ (1999) Single amino acid substitutions in α-conotoxin PnIA shift selectivity for subtypes of the mammalian neuronal nicotinic acetylcholine receptor. *J Biol Chem* **274:**36559–36564.
Hone AJ, Meyer EL, McIntyre M, and McIntosh JM (2012) Nicotinic acetylcholine receptors in dorsal root ganglion neurons include the α6β4* subtype. *FASEB J* **26:**917–926.
Hone AJ, Whiteaker P, Christensen S, Xiao Y, Meyer EL, and McIntosh JM (2009) A novel fluorescent α-conotoxin for the study of α7 nicotinic acetylcholine receptors. *J Neurochem* **111:**80–89.
Hu SH, Gehrmann J, Guddat LW, Alewood PF, Craik DJ, and Martin JL (1996) The 1.1 A crystal structure of the neuronal acetylcholine receptor antagonist, α-conotoxin PnIA from *Conus pennaceus*. *Structure* **4:**417–423.
Jackson KJ, McIntosh JM, Brunzell DH, Sanjakdar SS, and Damaj MI (2009) The role of α6-containing nicotinic acetylcholine receptors in nicotine reward and withdrawal. *J Pharmacol Exp Ther* **331:**547–554.
Jones IW and Wonnacott S (2004) Precise localization of α7 nicotinic acetylcholine receptors on glutamatergic axon terminals in the rat ventral tegmental area. *J Neurosci* **24:**11244–11252.
Kuryatov A and Lindstrom J (2011) Expression of functional human α6β2β3* acetylcholine receptors in *Xenopus laevis* oocytes achieved through subunit chimeras and concatamers. *Mol Pharmacol* **79:**126–140.
Kuryatov A, Olale F, Cooper J, Choi C, and Lindstrom J (2000) Human α6 AChR subtypes: subunit composition, assembly, and pharmacological responses. *Neuropharmacology* **39:**2570–2590.
Léna C, de Kerchove D'Exaerde A, Cordero-Erausquin M, Le Novère N, del Mar Arroyo-Jimenez M, and Changeux JP (1999) Diversity and distribution of nicotinic acetylcholine receptors in the locus ceruleus neurons. *Proc Natl Acad Sci USA* **96:**12126–12131.
Letchworth SR and Whiteaker P (2011) Progress and challenges in the study of α6-containing nicotinic acetylcholine receptors. *Biochem Pharmacol* **82:**862–872.
Liu L, Zhao-Shea R, McIntosh JM, Gardner PD, and Tapper AR (2012) Nicotine persistently activates ventral tegmental area dopaminergic neurons via nicotinic acetylcholine receptors containing α4 and α6 subunits. *Mol Pharmacol* **81:**541–548.
Luo S, Nguyen TA, Cartier GE, Olivera BM, Yoshikami D, and McIntosh JM (1999) Single-residue alteration in α-conotoxin PnIA switches its nAChR subtype selectivity. *Biochemistry* **38:**14542–14548.
Mao D, Yasuda RP, Fan H, Wolfe BB, and Kellar KJ (2006) Heterogeneity of nicotinic cholinergic receptors in rat superior cervical and nodose ganglia. *Mol Pharmacol* **70:**1693–1699.
Marritt AM, Cox BC, Yasuda RP, McIntosh JM, Xiao Y, Wolfe BB, and Kellar KJ (2005) Nicotinic cholinergic receptors in the rat retina: simple and mixed heteromeric subtypes. *Mol Pharmacol* **68:**1656–1668.
McIntosh JM, Azam L, Staheli S, Dowell C, Lindstrom JM, Kuryatov A, Garrett JE, Marks MJ, and Whiteaker P (2004) Analogs of α-conotoxin MII are selective for α6-containing nicotinic acetylcholine receptors. *Mol Pharmacol* **65:**944–952.
McIntosh JM, Plazas PV, Watkins M, Gomez-Casati ME, Olivera BM, and Elgoyhen AB (2005) A novel α-conotoxin, PeIA, cloned from *Conus pergrandis*, discriminates between rat α9α10 and α7 nicotinic cholinergic receptors. *J Biol Chem* **280:**30107–30112.
Moretti M, Vailati S, Zoli M, Lippi G, Riganti L, Longhi R, Viegi A, Clementi F, and Gotti C (2004) Nicotinic acetylcholine receptor subtypes expression during rat retina development and their regulation by visual experience. *Mol Pharmacol* **66:**85–96.
Papke RL, Buhr JD, Francis MM, Choi KI, Thinschmidt JS, and Horenstein NA (2005) The effects of subunit composition on the inhibition of nicotinic receptors by the amphipathic blocker 2,2,6,6-tetramethylpiperidin-4-yl heptanoate. *Mol Pharmacol* **67:**1977–1990.
Perez XA, Bordia T, McIntosh JM, Grady SR, and Quik M (2008) Long-term nicotine treatment differentially regulates striatal α6α4β2* and α6(nonα4)β2* nAChR expression and function. *Mol Pharmacol* **74:**844–853.
Pérez-Alvarez A, Hernández-Vivanco A, McIntosh JM, and Albillos A (2012) Native α6β4* nicotinic receptors control exocytosis in human chromaffin cells of the adrenal gland. *FASEB J* **26:**346–354.
Pivavarchyk M, Smith AM, Zhang Z, Zhou D, Wang X, Toyooka N, Tsuneki H, Sasaoka T, McIntosh JM, Crooks PA, et al. (2011) Indolizidine (−)-235B′ and related structural analogs: discovery of nicotinic receptor antagonists that inhibit nicotine-evoked [^{3}H]dopamine release. *Eur J Pharmacol* **658:**132–139.
Pons S, Fattore L, Cossu G, Tolu S, Porcu E, McIntosh JM, Changeux JP, Maskos U, and Fratta W (2008) Crucial role of α4 and α6 nicotinic acetylcholine receptor subunits from ventral tegmental area in systemic nicotine self-administration. *J Neurosci* **28:**12318–12327.
Pucci L, Grazioso G, Dallanoce C, Rizzi L, De Micheli C, Clementi F, Bertrand S, Bertrand D, Longhi R, De Amici M, et al.(2011) Engineering of α-conotoxin MII-derived peptides with increased selectivity for native α6β2* nicotinic acetylcholine receptors. *FASEB J* **25:**3775–3789.
Quik M, Polonskaya Y, Gillespie A, Jakowec M, Lloyd GK, and Langston JW (2000) Localization of nicotinic receptor subunit mRNAs in monkey brain by in situ hybridization. *J Comp Neurol* **425:**58–69.
Rogers JP, Luginbühl P, Shen GS, McCabe RT, Stevens RC, and Wemmer DE (1999) NMR solution structure of α-conotoxin ImI and comparison to other conotoxins specific for neuronal nicotinic acetylcholine receptors. *Biochemistry* **38:**3874–3882.
Vincler MA and Eisenach JC (2003) Immunocytochemical localization of the α3, α4,

α5, α7, β2, β3 and β4 nicotinic acetylcholine receptor subunits in the locus coeruleus of the rat. *Brain Res* **974:**25–36.

Wooltorton JR, Pidoplichko VI, Broide RS, and Dani JA (2003) Differential desensitization and distribution of nicotinic acetylcholine receptor subtypes in midbrain dopamine areas. *J Neurosci* **23:**3176–3185.

Wu J, George AA, Schroeder KM, Xu L, Marxer-Miller S, Lucero L, and Lukas RJ (2004) Electrophysiological, pharmacological, and molecular evidence for α7-nicotinic acetylcholine receptors in rat midbrain dopamine neurons. *J Pharmacol Exp Ther* **311:**80–91.

Yang K, Hu J, Lucero L, Liu Q, Zheng C, Zhen X, Jin G, Lukas RJ, and Wu J (2009) Distinctive nicotinic acetylcholine receptor functional phenotypes of rat ventral tegmental area dopaminergic neurons. *J Physiol* **587:**345–361.

Address correspondence to: Dr. J. Michael McIntosh, Department of Psychiatry, 50 North 1900, East Salt Lake City, UT 84132. E-mail: mcintosh.mike@gmail.com